

## Coordination Modes | *Hot Paper*

# Coordination Behavior of a P<sub>4</sub>-Butterfly Complex towards Transition Metal Lewis Acids: Preservation versus Rearrangement

Julian Müller and Manfred Scheer\*<sup>[a]</sup>

Dedicated to Professor Gerhard Erker on the occasion of his 75th birthday.

**Abstract:** The reactivity of the P<sub>4</sub> butterfly complex  $[(\text{Cp}^{\text{III}}\text{Fe}(\text{CO})_2)_2(\mu_3, \eta^{1:1:1}\text{-P}_4)]$  (**1**, Cp<sup>III</sup> = η<sup>5</sup>-C<sub>5</sub>H<sub>2</sub>tBu<sub>3</sub>) towards divalent Co, Ni and Zn salts is investigated. The reaction with the bromide salts leads to  $[(\text{Cp}^{\text{III}}\text{Fe}(\text{CO})_2)_2(\mu_3, \eta^{2:1:1}\text{-P}_4)]\{\text{MBr}_2\}$  (M = Co (**2Co**), Ni (**2Ni**), Zn (**2Zn**)) in which the P<sub>4</sub> butterfly scaffold is preserved. The use of the weakly ligated Co complex  $[\text{Co}(\text{NCCH}_3)_6][\text{SbF}_6]_2$ , results in the formation of  $[(\text{Cp}^{\text{III}}\text{Fe}(\text{CO})_2)_2(\mu_3, \eta^{4:1:1}\text{-P}_4)]_2\text{Co}][\text{SbF}_6]_3$  (**3**), which represents the second example of a homoleptic-like octaphospha-metalla-sandwich complex. The formation of the threefold positively charged complex **3** occurs via redox processes, which among others also enables the formation of  $[(\text{Cp}^{\text{III}}\text{Fe}(\text{CO})_2)_4(\mu_5, \eta^{4:1:1:1:1}\text{-P}_4)]\{\text{Co}(\text{CO})_2\}][\text{SbF}_6]$  (**4**), bearing a rare octaphosphabicyclo[3.3.0]octane unit as a ligand. On the other hand, the reaction with  $[\text{Zn}(\text{NCCH}_3)_4][\text{PF}_6]_2$  yields the spiro complex  $[(\text{Cp}^{\text{III}}\text{Fe}(\text{CO})_2)_2(\mu_3, \eta^{2:1:1}\text{-P}_4)]_2\text{Zn}][\text{PF}_6]_2$  (**5**) under preservation of the initial structural motif.

sis.<sup>[2,3,10]</sup> Compounds with a higher phosphorus content show an even more diverse coordination chemistry. For example, the monoanionic P<sub>3</sub> chain  $[\text{tBu}_2\text{P-P-PtBu}_2]^-$  is able to coordinate up to two  $[\text{Cr}(\text{CO})_4]$  fragments in an η<sup>2:1</sup> fashion,<sup>[11]</sup> while linear tetraphosphides can undergo a [4 + 1] cycloaddition to give five membered metallacycles.<sup>[12]</sup> Furthermore, cyclic systems of tetraphosphines<sup>[13]</sup> and pentaphosphines<sup>[14]</sup> can also act as bidentate ligands. Here, regardless of the ring size, the oligophosphines always stabilize the metal center in a 1,3-coordination mode. However, the highest diversity of coordination modes is found for phosphorus ligands that do not bear any organic substituents.<sup>[1]</sup> These so called P<sub>n</sub> ligands are usually obtained by reactions of white phosphorus (P<sub>4</sub>) with either main group or transition metal moieties.<sup>[15]</sup> One of the first steps in the activation of the tetrahedral P<sub>4</sub> molecule is the formation of a tetraphosphabicyclo[1.1.0]butane unit<sup>[16,17]</sup> which can be stabilized by forming either mononuclear<sup>[16,18]</sup> or binuclear<sup>[19–22]</sup> P<sub>4</sub> butterfly complexes.

Our group could show that the P<sub>4</sub> butterfly complex  $[(\text{Cp}^{\text{III}}\text{Fe}(\text{CO})_2)_2(\mu_3, \eta^{1:1:1}\text{-P}_4)]$  (**1**, Cp<sup>III</sup> = η<sup>5</sup>-C<sub>5</sub>H<sub>2</sub>tBu<sub>3</sub>) also fulfils the requirements of a bidentate ligand (Figure 1, top left), which mimics the dppm ligand.<sup>[23,24]</sup> In **1**, the central P<sub>4</sub> butterfly unit coordinates the Lewis acids via its two “wing-tip” phosphorus atoms. This results in complexes that can best be compared with the corresponding dppm complexes since they exhibit a very similar geometry, steric bulk and bite angle. However, in contrast to dppm, we could also show that **1** is electronically very flexible. On the one hand, **1** can act as a 4σ-electron donor. This is demonstrated in the case of  $[\text{Cu}(\text{NCCH}_3)_4][\text{BF}_4]$ , where the monoadduct  $[(\text{Cp}^{\text{III}}\text{Fe}(\text{CO})_2)_2(\mu_3, \eta^{2:1:1}\text{-P}_4)]\{\text{Cu}(\text{NCCH}_3)\}[\text{BF}_4]$  (**A**) as well as the spiro compound  $[(\text{Cp}^{\text{III}}\text{Fe}(\text{CO})_2)_2(\mu_3, \eta^{2:1:1}\text{-P}_4)]_2\text{Cu}][\text{BF}_4]$  (**B**) can be obtained, depending on the stoichiometry (Figure 1).<sup>[23]</sup> On the other hand, reactivity studies with Fe<sup>II</sup> salts have shown that the reaction outcome is strongly dependent on the nature of the ligands since the ligands influence the electron affinity of the metal center. Therefore, the reaction with  $[\text{FeBr}_2\text{-dme}]$  (dme = dimethoxyethane) yields the neutral coordination compound  $[(\text{Cp}^{\text{III}}\text{Fe}(\text{CO})_2)_2(\mu_3, \eta^{2:1:1}\text{-P}_4)]\{\text{FeBr}_2\}$  (**C**).<sup>[24]</sup> However, performing the same reaction in the presence of an Fe<sup>II</sup> salt with more labile acetonitrile ligands, an isomerization of the butterfly unit to an aromatic *cyclo*-P<sub>4</sub>[Fe]<sub>2</sub> entity ( $[\text{Fe}] = [\text{Cp}^{\text{III}}\text{Fe}(\text{CO})_2]$ ) is observed, which now acts as a 6π-electron donor (Figure 1, top right). This leads to the formation of the first octaphosphorus-iron-sandwich complex  $[(\text{Cp}^{\text{III}}\text{Fe}(\text{CO})_2)_2(\mu_3, \eta^{4:1:1}\text{-P}_4)]_2\text{Fe}][\text{PF}_6]_2$  (**D**). The conditions of the isomerization of **1** are still not fully understood. However, the results

## Introduction

Oligophosphorus compounds are a versatilely useable class of compounds and are therefore in the focus of current research. As they typically exhibit several sterically accessible lone pairs, these compounds show a manifold coordination chemistry.<sup>[1–3]</sup> Some of the most prominent representatives are the bis(diphenyl)phosphines of the type Ph<sub>2</sub>P(CH<sub>2</sub>)<sub>n</sub>PPh<sub>2</sub> (dppm, *n* = 1; dppe, *n* = 2; dppp, *n* = 3) that can act as monodentate,<sup>[4]</sup> chelating bidentate<sup>[5–9]</sup> or non-chelating bidentate<sup>[6,9]</sup> ligands. Due to their preference to form chelate complexes with small bite angles, these ligands are especially useful in homogeneous cataly-

[a] J. Müller, Prof. M. Scheer  
University of Regensburg  
Institute of Inorganic Chemistry  
93040 Regensburg (Germany)  
E-mail: Manfred.Scheer@ur.de

Supporting information and the ORCID identification number(s) for the author(s) of this article can be found under:  
<https://doi.org/10.1002/chem.202005025>.

© 2020 The Authors. Published by Wiley-VCH GmbH. This is an open access article under the terms of the Creative Commons Attribution Non-Commercial NoDerivs License, which permits use and distribution in any medium, provided the original work is properly cited, the use is non-commercial and no modifications or adaptations are made.

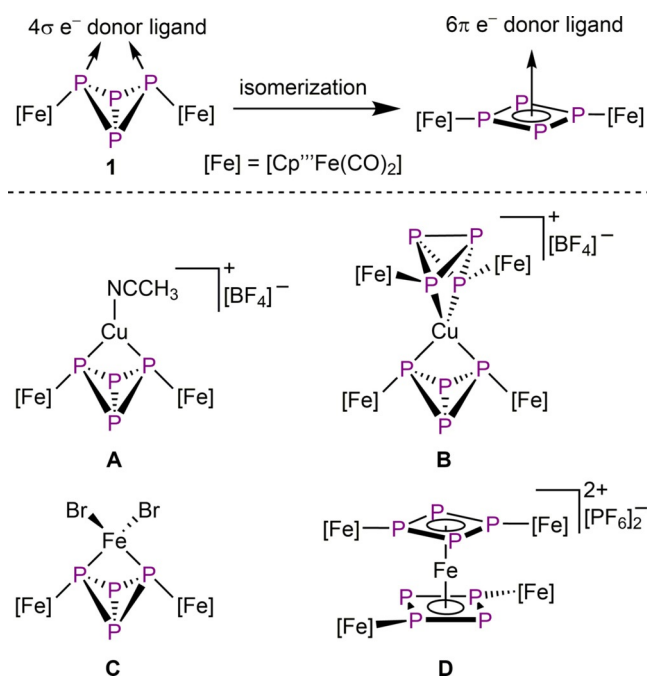


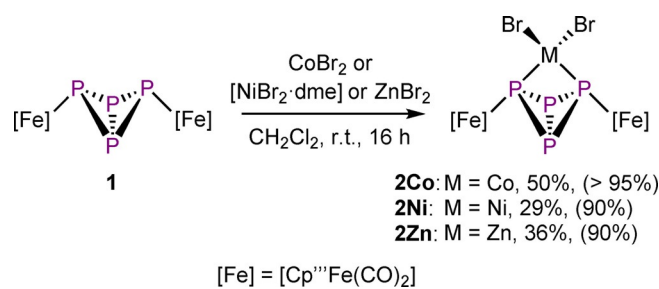
**Figure 1.** Top: Schematic illustration of the isomerization of  $[(\text{Cp}^*\text{Fe}(\text{CO})_2)_2(\mu_3, \eta^{11}\text{-P}_4)]$  (**1**). Bottom: Examples of coordination compounds **A–D** synthesized from **1**.

with  $\text{Fe}^{\text{II}}$  have shown, that the reactivity is strongly dependent on the nature of the ligands of the Lewis acid. To investigate this phenomenon further and to rationalize under what conditions what kind of coordination behavior is to be expected, we investigated the reaction of the butterfly complex **1** with various divalent transition metal compounds.

Herein, we report on detailed studies of the coordination behavior of the butterfly complex **1** towards 3d transition metal-based Lewis acids. A preservation of the  $\text{P}_4$  butterfly framework is observed in most of the reactions. However, it could also be shown that **1** has a high tendency to rearrange in the presence of weakly ligated  $d^6$  metals, which yields complexes that contain  $\text{cyclo-P}_4[\text{Fe}]_2$  units ( $[\text{Fe}] = \text{Cp}^*\text{Fe}(\text{CO})_2$ ) or the rare octaphosphabicyclo[3.3.0]octane unit as ligands.

## Result and Discussion

The reactions of **1** with 1.1 equivalents of the divalent bromide salts  $\text{CoBr}_2$ ,  $[\text{NiBr}_2\text{-dme}]$  or  $\text{ZnBr}_2$  lead to the formation of  $[(\text{Cp}^*\text{Fe}(\text{CO})_2)_2(\mu_3, \eta^{11}\text{-P}_4)\{\text{MBr}_2\}]$  ( $\text{M} = \text{Co}$  (**2Co**), Ni (**2Ni**), Zn (**2Zn**)), respectively, which can be isolated in moderate crystalline yields (Scheme 1). The molecular structures of **2Co**, **2Ni** and **2Zn** (Figures 2, S2 and S3) reveal that the  $\text{P}_4$  butterfly unit is still intact and coordinates the Lewis acidic metal atom always via the two “wing-tip” phosphorus atoms. The metal centers are coordinated in a distorted tetrahedral fashion, which is indicated by the twist angles of the  $\text{P1-M1-P2}$  plane to the  $\text{Br1-M1-Br2}$  plane of  $86.15(1)^\circ$  (**2Co**),  $84.39(4)^\circ$  (**2Ni**) and  $85.92(2)^\circ$  (**2Zn**), respectively. The trend in the covalence radii<sup>[25]</sup> of Fe ( $r_{\text{Fe}} = 1.16 \text{ \AA}$ ), Co ( $r_{\text{Co}} = 1.11 \text{ \AA}$ ), Ni ( $r_{\text{Ni}} = 1.10 \text{ \AA}$ ) and Zn ( $r_{\text{Zn}} = 1.18 \text{ \AA}$ ) is nicely reflected in the metal phosphorus bond



**Scheme 1.** Syntheses of the coordination compounds with divalent bromide salts starting from **1**. The displayed yields correspond to the isolated crystalline yield referred to **1**. The number in brackets gives the yield according to the  $^{31}\text{P}$  NMR spectroscopy of the reaction mixtures.

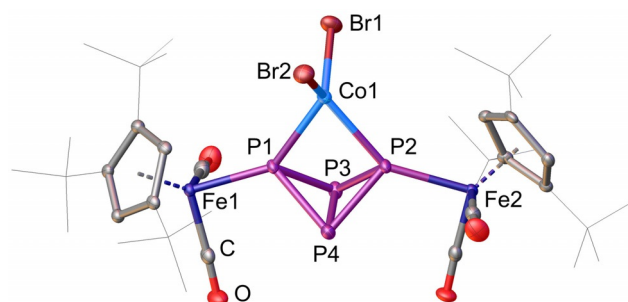


**Figure 2.** Molecular structure of **2Co** in the solid state exemplifying the structural core of **2Ni** and **2Zn** as well (cf. Figures S2 and S3). Hydrogen atoms and  $\text{CH}_2\text{Cl}_2$  molecules are omitted for clarity. Atom displacement parameters (ADPs) are shown at 50% probability level.

lengths of **C** ( $2.4364(7)/2.4823(8) \text{ \AA}$ )<sup>[24]</sup> **2Co** ( $2.3614(11)/2.3959(11) \text{ \AA}$ ), **2Ni** ( $2.3389(15)/2.3607(14) \text{ \AA}$ ), **2Zn** ( $2.4479(6)/2.5002(6) \text{ \AA}$ ). However, the P–Ni bond lengths of **2Ni** are longer compared to the ones in the square planar complex  $[(\text{dppm})\text{NiBr}_2]$  ( $2.143(2) \text{ \AA}$  and  $2.152(2) \text{ \AA}$ ).<sup>[8]</sup> The deviation of the geometry of the nickel center ( $d^8$  configuration) from the preferred square planar geometry ( $[(\text{dppm})\text{NiBr}_2]$ ) to a distorted tetrahedral geometry (**2Ni**) must be caused by the steric bulk of **1** that does not allow a square planar geometry at the nickel atom. With  $70.102(18)^\circ$  the bite angle of the  $\text{P}_4$  butterfly unit in **2Zn** is almost identical with the corresponding angle in **C** ( $70.27(3)^\circ$ ).<sup>[24]</sup> The cobalt and nickel analogues exhibit a slightly larger bite angle of  $73.55(4)^\circ$  (**2Co**) and  $72.08(5)^\circ$  (**2Ni**). However, the bite angle in **2Ni** is smaller compared to the one in  $[(\text{dppm})\text{NiBr}_2]$  ( $75.62(8)^\circ$ ).<sup>[8]</sup> In all three compounds the P–P bond lengths are in the range of a common P–P single bond as it was observed for **C**.<sup>[24]</sup>

The  $^1\text{H}$  NMR spectra ( $\text{CD}_2\text{Cl}_2$ ) of **2Co**, **2Ni** and **2Zn** each show three signals for the two magnetically equivalent  $\text{Cp}^*$  ligands. The  $^1\text{H}$  NMR spectrum of **2Zn** reveals two broad singlets at  $\delta = 1.42 \text{ ppm}$  and  $\delta = 1.37 \text{ ppm}$  with an integral ratio of 18:9 which can be assigned to the three *t*Bu groups. The broad signal with an integral of 2 at  $\delta = 5.11 \text{ ppm}$  can be assigned to the two aryl H atoms of the  $\text{Cp}^*$  ligands. Since compound **2Co** and **2Ni** are paramagnetic, the signals in the  $^1\text{H}$  NMR spectra are strongly shifted. The  $^1\text{H}$  NMR spectrum of **2Co** exhibits three broad signals at  $\delta = -3.7$ ,  $-5.8$  and  $-26.1 \text{ ppm}$  with an

integral ratio of 18:9:2. In the case of **2Ni**, the signals with an integral ratio of 9:18:2 are shifted to  $\delta=3.9$ , 3.3 and  $-15.8$  ppm, respectively.

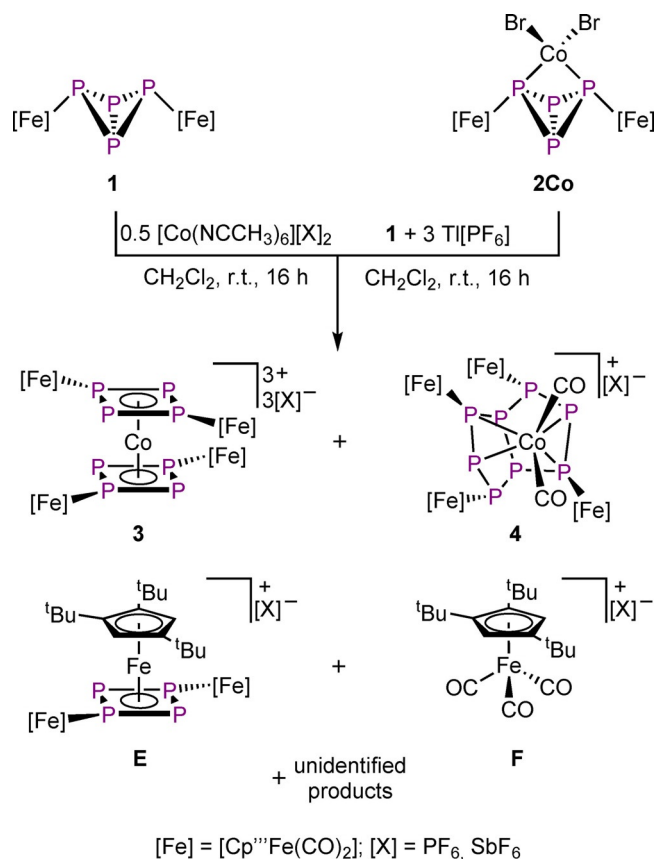
The  $^{31}\text{P}\{^1\text{H}\}$  NMR spectrum of **2Zn** in  $\text{CD}_2\text{Cl}_2$  reveals two sharp triplets of an  $A_2X_2$  spin system at  $\delta=-43.1$  ppm and  $\delta=-309.6$  ppm ( $J_{\text{PP}}=198$  Hz). In comparison to the chemical shifts of **2Zn**, the signals of **1** ( $\delta=-81.4$  ppm and  $\delta=-325.0$  ppm)<sup>[19,22]</sup> and **A** ( $\delta=-73.2$  ppm and  $\delta=-313.7$  ppm)<sup>[23]</sup> are shifted to lower ppm values.

The  $^{31}\text{P}\{^1\text{H}\}$  NMR spectrum ( $\text{CD}_2\text{Cl}_2$ ) of the reaction solution of **2Zn** reveals an additional set of signals at  $\delta=137.3$ , 69.3 and 16.0 ppm corresponding to a byproduct (coupling constants are summarized in Table S4).<sup>[24,26]</sup> The integral ratio of main product to side product is 10:1. Despite several attempts, the exact structure of this byproduct could not be clarified yet, but according to the chemical shift as well as the coupling pattern, the presence of a *cyclo*- $\text{P}_4$  unit is very likely. The formation of this byproduct may be attributed to a partial fragmentation of **1** as this can generate metal species that can be coordinated by **1**. The formation of *cyclo*- $\text{P}_4$  containing complexes, induced by a partial fragmentation of **1**, has already been observed.<sup>[24]</sup>

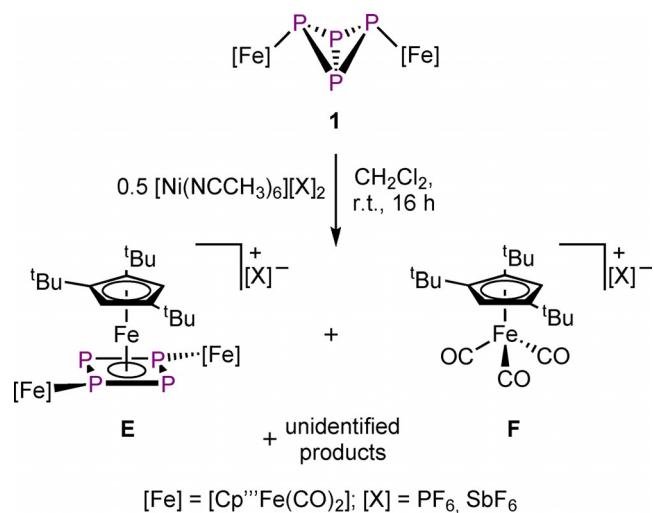
The  $^{31}\text{P}\{^1\text{H}\}$  NMR spectrum of **2Ni** in  $\text{CD}_2\text{Cl}_2$  shows only one very broad signal at  $\delta=-267.3$  ppm ( $\omega_{1/2}=575$  Hz) while **2Co** is  $^{31}\text{P}$  NMR silent. During the synthesis of **2Ni** a diamagnetic byproduct is formed which can be observed in the  $^{31}\text{P}\{^1\text{H}\}$  NMR spectrum ( $\text{CD}_2\text{Cl}_2$ ) of the reaction solution in form of an  $AA'XX'$  spin system at  $\delta=97.4$  ppm and 198.8 ppm. The corresponding coupling constants are summarized in Table S3. The chemical shifts and coupling pattern point towards the presence of a cyclic  $\text{P}_4$  unit instead of a  $\text{P}_4$ -butterfly core. Regardless of numerous attempts, the nature of the byproduct could not be unambiguously clarified so far.

Although **2Co** and **2Ni** are paramagnetic, they are EPR silent, indicating the presence of high spin  $d^7$  and  $d^8$  configurations, respectively. The same behavior was observed for complex **C** where a high spin  $d^6$  configuration could be verified for the central iron atom.<sup>[24]</sup> According to the applied Evans method<sup>[27]</sup> compound **2Co** possesses an effective magnetic moment of  $\mu_{\text{eff}}=4.8 \mu_{\text{B}}$ . Although the value is higher than  $3.9 \mu_{\text{B}}$ , which is expected for three unpaired electrons, it is in good agreement with experimentally found values of tetrahedrally coordinated  $\text{Co}^{\text{II}}$  complexes ( $\mu_{\text{eff}}=4.3\text{--}4.7 \mu_{\text{B}}$ ).<sup>[28]</sup> Complex **2Ni** exhibits an effective magnetic moment of  $\mu_{\text{eff}}=2.7 \mu_{\text{B}}$  that fits to two unpaired electrons. However, this value is smaller compared to other tetrahedrally coordinated  $\text{Ni}^{\text{II}}$  compounds that have magnetic moments within the range of  $\mu_{\text{eff}}=3.3\text{--}4.0 \mu_{\text{B}}$ .<sup>[29]</sup> On the other hand, complexes of  $[\text{NiX}_2\text{L}]$  ( $\text{X}=\text{Cl}, \text{Br}, \text{I}$ ;  $\text{L}=\text{bis-diphosphines}$ ) are mainly described to be diamagnetic caused by the square planar geometry.<sup>[7,8,30]</sup>

The unexpected formation of the sandwich complex **D** in the reaction of **1** with  $[\text{Fe}(\text{NCCH}_3)_6][\text{PF}_6]_2$ <sup>[24]</sup> inspired us to investigate the reaction of **1** with  $\text{M}^{\text{II}}$  compounds containing labile ligands. Therefore, we reacted two equivalents of **1** with 1.05 equivalents of  $[\text{M}(\text{NCCH}_3)_n][\text{X}]_2$  ( $\text{M}=\text{Co}$ ,  $n=6$ ,  $\text{X}=\text{PF}_6$ ,  $\text{SbF}_6$ , Scheme 2;  $\text{M}=\text{Ni}$ ,  $n=6$ ,  $\text{X}=\text{PF}_6$ ,  $\text{SbF}_6$ , Scheme 3;  $\text{M}=\text{Zn}$ ,  $n=4$ ,  $\text{X}=\text{PF}_6$ , Scheme 4).

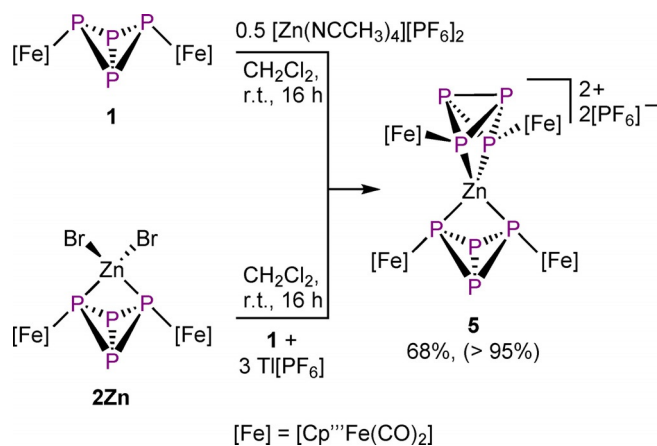


**Scheme 2.** Coordination complexes derived from **1** in the presence of labile ligated cobalt centers.



**Scheme 3.** Coordination complexes derived from **1** in the presence of  $[\text{Ni}(\text{NCCH}_3)_6][\text{X}]_2$  ( $\text{X}=\text{PF}_6, \text{SbF}_6$ ).

Based on  $^{31}\text{P}$  NMR spectroscopic investigations, the reaction of **1** with  $[\text{Co}(\text{NCCH}_3)_6][\text{X}]_2$  ( $\text{X}=\text{PF}_6, \text{SbF}_6$ ) leads to the formation of a variety of products (Scheme 2). The use of the salt with the better soluble hexafluorophosphate anion only allowed the characterization of the already known compounds  $[\{\text{Cp}^{\text{III}}\text{Fe}(\text{CO})_2\}_2(\mu_3, \eta^{4:1:1}\text{-P}_4)(\text{Cp}^{\text{III}}\text{Fe})][\text{PF}_6]_2$ <sup>[24]</sup> (**E**) and  $[\text{Cp}^{\text{III}}\text{Fe}(\text{CO})_3][\text{PF}_6]$  (**F**) by single crystal X-ray structure analysis,  $^{31}\text{P}$  NMR



**Scheme 4.** Coordination complexes derived from **1** in the presence of the labile ligated Lewis acid of zinc. The displayed yields correspond to the isolated crystalline yield referred to **1**. The number in brackets gives the yield according to the  $^{31}\text{P}$  NMR spectroscopy of the reaction mixtures.

spectroscopy and mass spectrometry (see supporting information). However, switching to the less soluble hexafluoroantimonate anion additionally allows the isolation of  $[\{(\text{Cp}''\text{Fe}(\text{CO})_2)_2(\mu_3, \eta^{4:1:1}\text{-P}_4)_2\text{Co}\}[\text{SbF}_6]_3$  (**3**) (3%) and few crystals of  $[\{(\text{Cp}''\text{Fe}(\text{CO})_2)_4(\mu_5, \eta^{4:1:1:1:1}\text{-P}_8)\{\text{Co}(\text{CO})_2\}[\text{SbF}_6]_4$  (**4**). The central  $\text{P}_8$  unit of **4** is a rare example of an octaphosphabicyclo[3.3.0]octane unit which must have been formed by a dimerization of **1** in the presence of a  $[\text{Co}(\text{CO})_2]^{3+}$  unit. Complex **3** however, contains two *cyclo*- $\text{P}_4[\text{Fe}]_2$  units that coordinate the central cobalt atom in an  $\eta^4$  coordination mode each. Therefore, **3** represents the second example of a homoleptic-like octaphospha-metalla-sandwich complex.<sup>[24]</sup> The threefold positive charge of **3** indicates that the central cobalt atom must be in the oxidation state of +III. Hence, **3** is isoelectronic to **D**,<sup>[24]</sup> which shows that the isomerization has a high tendency to occur in the presence of weakly ligated  $d^6$  metals. The charge of the complex also reveals that redox processes are involved in the formation of **3**. Surprisingly, the cyclic voltammogram of  $[\text{Co}(\text{NCCH}_3)_6][\text{PF}_6]_2$  in  $\text{CH}_2\text{Cl}_2$  reveals that the  $\text{Co}^{2+}$  ion can only be reduced electrochemically, but not oxidized (Figure S33). On the other hand, **1** can be both oxidized and reduced electrochemically but both processes are irreversible (Figure S34). Therefore, the  $\text{Co}^{3+}$  ion is most likely produced chemically by a reduction of **1** during the reaction. However, the use of an excess of **1** as well as the addition of  $[\text{Cp}_2\text{Fe}][\text{PF}_6]$  as an electron acceptor did not enhance the formation of **3** significantly. The driving force for this oxidation is most likely the isomerization of the butterfly units to the aromatic *cyclo*- $\text{P}_4[\text{Fe}]_2$  units (see Figure 1, top), since DFT calculations showed that the analogue reaction of  $[\text{Fe}(\text{NCCH}_3)_6]^{2+}$  and **1** is exothermic by  $-118.76 \text{ kJ mol}^{-1}$ .<sup>[24]</sup> The redox processes must also induce a degradation of **1**, since all characterized side products indicate a partial decomposition of **1**. The tendency of butterfly complexes to decompose and rearrange in the presence of reactive species or under harsh reaction conditions has already been discussed in the literature.<sup>[19,20,24]</sup> Despite intensive efforts it was not possible to identify other products of this reaction that would allow a better insight into the reaction pathway.

This is mainly hindered by the very similar solubility of all the products since all are charged and bear the well soluble  $\text{Cp}''$  ligand.

The single-crystal X-ray structure analysis of **3** reveals that the  $\text{P}_4$  butterfly units have isomerized into *cyclo*- $\text{P}_4$  units that coordinate as 6  $\pi$ -electron donors to the central Co atom (Figure 3). The P–P bond lengths vary from 2.135(2) to 2.154(2) Å and are between a P–P single ( $\approx 2.22$  Å)<sup>[25]</sup> and a P=P double bond ( $\approx 2.04$  Å).<sup>[31]</sup> Compared to other *cyclo*- $\text{P}_4^{2-}$  containing compounds, the P–P bond lengths of **3** are in good agreement.<sup>[24,32,33]</sup> The geometry of the *cyclo*- $\text{P}_4$  units is with P–P–P angles from 83.17(8) to 96.62(8)° slightly distorted compared to the square  $\text{P}_4^{2-}$  anion of  $[\text{Cs}_2\text{P}_4 \cdot 2\text{NH}_3]$  (89.76(4) and 90.24(4)°).<sup>[33]</sup> The deformation is most likely induced by the two sterically demanding [Fe] fragments that stabilize each *cyclo*- $\text{P}_4$  unit. However, compared to the analogue iron complex **D**,<sup>[24]</sup> the P–P angles of **3** are slightly closer to the ideal value of 90°. The planar  $\text{P}_4$  rings in **3** (sums of the P–P–P angles are 359.95 and 359.96°) are almost parallel with an  $\text{P}_{4,\text{cent}}\text{-Co-P}_{4,\text{cent}}$  angle of 178.00(7)°. The two *cyclo*- $\text{P}_4$  units are in an eclipsed conformation while **D** shows an intermediate state between the staggered and the eclipsed conformation.<sup>[24]</sup> However, DFT calculations have predicted that the hypothetical  $[(\text{P}_4)_2\text{Co}^{\text{III}}]^-$  anion containing square *cyclo*- $\text{P}_4$  ligands has a staggered conformation ( $D_{4d}$  symmetry).<sup>[34]</sup> The Fe–P distances vary from 2.1972(17) to 2.2055(17) Å and are shorter than the corresponding distances in **D** (2.2255(9) to 2.2317(9) Å)<sup>[24]</sup> and **1** (2.348(2) and 2.3552(19) Å).<sup>[19]</sup>

The  $^1\text{H}$  NMR spectrum ( $\text{CD}_3\text{CN}$ ) of **3** shows three broad signals for the magnetically equivalent  $\text{Cp}''$  ligands at  $\delta = 6.01$ , 1.44 and 1.39 ppm with an integral ratio of 2:9:18. The  $^{31}\text{P}\{^1\text{H}\}$  NMR spectrum ( $\text{CD}_3\text{CN}$ ) of **3** reveals an AA'XX' spin system at  $\delta = 196.8$  and 144.1 ppm (coupling constants are summarized

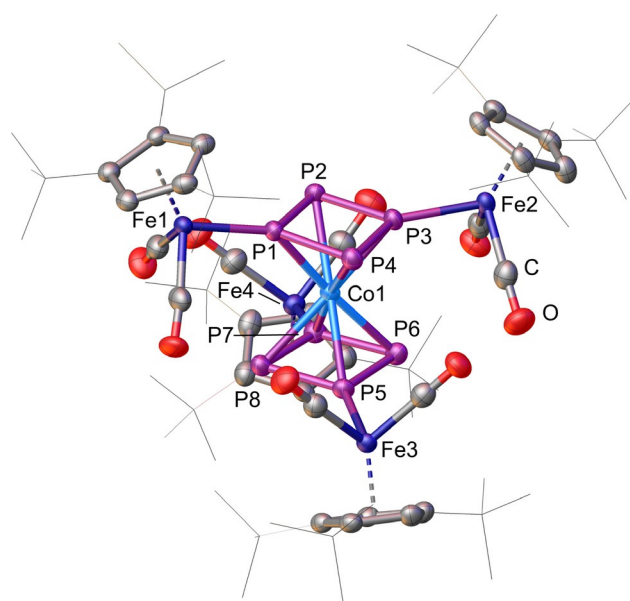


**Figure 3.** Cationic part of the molecular structure of **3**. The three  $\text{SbF}_6^-$  anions, hydrogen atoms and solvent molecules are omitted for clarity. ADPs are shown at 50% probability level.

in Table S5). Compared to the iron containing complex **D** ( $\delta = 114.3$  and  $91.7$  ppm in  $\text{CD}_2\text{Cl}_2$ )<sup>[24]</sup> the signals of **3** are strongly shifted downfield.

The molecular structure of **4** reveals the formation of a mono-cationic complex that contains an octaphospha-bicyclo[3.3.0]octane cage (Figure 4), which can be derived from the realgar structure type with a  $[\text{Co}(\text{CO})_2]^{3+}$  fragment inserted into the P4–P8 bond. The  $\text{P}_8$  unit can also be described as two fused  $\text{P}_5$  rings that are twisted due to the coordination of the  $[\text{Co}(\text{CO})_2]^{3+}$  fragment. The only comparable complex with a yet more symmetrical  $\text{P}_8$  unit is  $[\text{K}(\text{dme})_2][(\text{Cp}^*\text{Co})_2(\mu_3\eta^{3,3}\text{-P}_8)]$ .<sup>[35]</sup> However, the dicobalt complex consists of two allylic subunits (P–P bond length of  $2.1519(6)$ – $2.1580(6)$  Å) that are connected via P–P single bonds ( $2.1947(6)$ – $2.2247(6)$  Å),<sup>[35]</sup> while the P–P bond lengths in **4** vary from  $2.1928(17)$  Å to  $2.2308(18)$  Å. The only exceptions are the P1–P8 ( $2.116(2)$  Å) and P4–P5 ( $2.111(2)$  Å) bonds that are shorter due to the side-on coordination of the cobalt atom. The four Co–P bond lengths in **4** are not equal. The distances to the phosphorus atoms that are also coordinated by an iron fragment are shorter (Co1–P1 ( $2.2553(1)$  Å), Co1–P5 ( $2.2551(17)$  Å) compared to the substituent free P atoms P4 ( $2.4058(18)$  Å) and P8 ( $2.4098(17)$  Å). The Fe–P distances vary from  $2.2996(15)$  Å to  $2.3115(15)$  Å and are slightly shortened compared to the ones in **1**.<sup>[19]</sup>

The question whether the central  $[\text{M}(\text{CO})_2]$  fragment in **4** contains an iron or a cobalt atom cannot be unambiguously clarified by single crystal structure analysis. Therefore, a solution of **4** was investigated by ESI mass spectrometry, where the presence of cobalt was confirmed by the detection of the molecular ion peak at  $m/z = 1743.4$ . The  $^{31}\text{P}\{^1\text{H}\}$  NMR spectrum of **4** in  $\text{thf-d}_8$  shows an AA'MM'OO'XX' spin system at  $\delta = 303.9$ ,

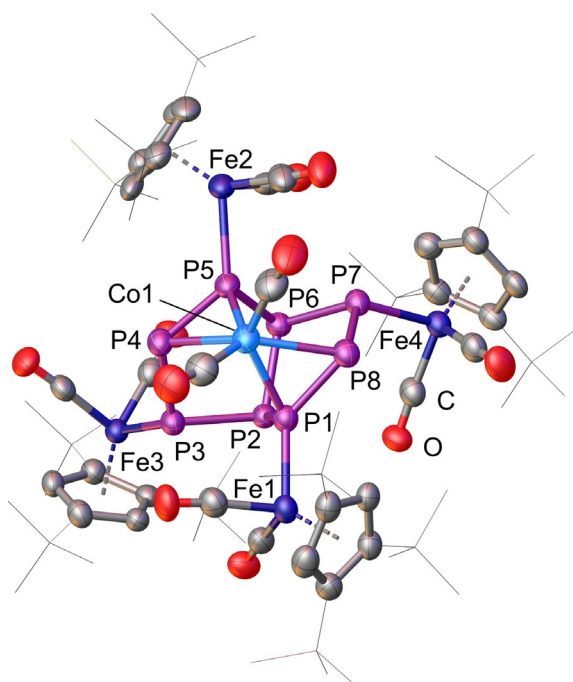


**Figure 4.** Cationic part of the molecular structure of **4**. The  $\text{SbF}_6^-$  anion and hydrogen atoms are omitted for clarity. ADPs are shown at 50% probability level.

$234.2$ ,  $-151.4$  and  $-272.9$  ppm (coupling constants are summarized in Table S6). Due to the diamagnetic nature of **4**, it can be concluded that **4** also contains cobalt in the oxidation state +III, which means that the ligand constitutes a  $\text{P}_8^{6-}$  unit.

Since the reaction of **1** with  $[\text{Co}(\text{NCCH}_3)_6][\text{X}]_2$  ( $\text{X} = \text{PF}_6, \text{SbF}_6$ ) leads to the formation of several side products, we investigated if the selectivity is increased when starting the reaction with compound **2Co** (Scheme 2). Therefore, **2Co** was treated with **1** and an excess (3 equivalents) of  $\text{Ti}[\text{PF}_6]$  in order to eliminate the two bromido ligands by the formation of  $\text{TIBr}$ . This should lead to vacancies in the coordination sphere of the  $\text{Co}^{\text{II}}$  center while it is still bound to **1**. However, the  $^{31}\text{P}\{^1\text{H}\}$  NMR spectrum of the reaction mixture indicates that this alternative reaction pathway does not lead to an increased selectivity, since the obtained NMR spectrum is comparable to the one of the reaction of **1** with  $[\text{Co}(\text{NCCH}_3)_6][\text{X}]_2$ .

The reaction of **1** with  $[\text{Ni}(\text{NCCH}_3)_6][\text{X}]_2$  ( $\text{X} = \text{PF}_6, \text{SbF}_6$ ) leads also to the formation of several products (Scheme 3;  $^{31}\text{P}\{^1\text{H}\}$  NMR of the reaction mixture is depicted in Figure S27). Despite several attempts, only the nickel-free fragmentation products **E** and **F** could be isolated and characterized, which were also observed in the analogue reaction with  $[\text{Co}(\text{NCCH}_3)_6][\text{X}]_2$ . The appearance of these degradation products indicates that **1** partially decomposes during the reaction with  $[\text{Ni}(\text{NCCH}_3)_6][\text{X}]_2$  which might also be induced by redox processes.

In contrast, stirring **1** with  $[\text{Zn}(\text{NCCH}_3)_4][\text{PF}_6]_2$  leads to the quantitative formation of  $[\{(\text{Cp}^*\text{Fe}(\text{CO})_2)_2(\mu_3\eta^{2,1,1}\text{-P}_4)_2\}\text{Zn}][\text{PF}_6]_2$  (**5**; Scheme 4; 68%, >95% according to  $^{31}\text{P}$  NMR spectroscopy). The spiro complex **5** bears two still intact  $\text{P}_4$  butterfly units that coordinate the central zinc atom. The preservation of the  $\text{P}_4$  butterfly scaffold can be explained by the electronic properties of  $\text{Zn}^{\text{II}}$  that has a  $d^{10}$  configuration. Therefore, the isomerization to *cyclo*- $\text{P}_4$  units ( $6\pi$ -electron donors) is not expected, but the preservation of the  $\text{P}_4$  butterfly scaffold ( $4\sigma$ -electron donor) enables the formation of a stable 18 valence electron complex. The existence of such spiro complexes was already observed for **B**.<sup>[23]</sup>

The molecular structure of **5** reveals that the central  $\text{Zn}^{2+}$  cation is coordinated by two butterfly units (Figure 5). The distorted tetrahedral geometry at  $\text{Zn1}$  is indicated by a twist angle of the  $\text{Zn1-P1-P2}$  plane to the  $\text{Zn1-P1'-P2}'$  plane of  $75.5814(5)^\circ$ . This twist angle is slightly larger than the one in **B** ( $74.882(2)^\circ$ )<sup>[23]</sup> but much smaller than the one in  $[\text{Zn}\{\eta^2\text{-}((\text{P}(i\text{Pr})_2)_2\text{N})_2\}]$  ( $87.53(5)^\circ$ ).<sup>[36]</sup> The Zn–P bond lengths of  $2.4471(11)$  and  $2.4536(11)$  Å are in good agreement with the ones of complex **2Zn** ( $2.4479(6)$ ,  $2.5002(6)$  Å). The bite angle of  $73.34(3)^\circ$  is approx.  $3^\circ$  larger compared to **2Zn** which can be explained by the steric repulsion of the four [Fe] fragments. With  $2.2102(15)$ – $2.2252(15)$  Å the distances between the “wing-tip” and the “bridge-head” P atoms are in the region of P–P single bonds, while the P3–P4 bond ( $2.1803(16)$  Å) has a slight double bond character. Compared to **1**,<sup>[19]</sup> the P–P bond lengths are slightly elongated which indicates a widening of the  $\text{P}_4$  butterfly scaffold during coordination of the  $\text{Zn}^{2+}$  cation. At the same time, the Fe–P distances ( $2.2806(12)$ ,  $2.2832(12)$  Å) are slightly shortened compared to the free ligand complex **1** ( $2.348(2)$ ,  $2.3552(19)$  Å).<sup>[19]</sup>

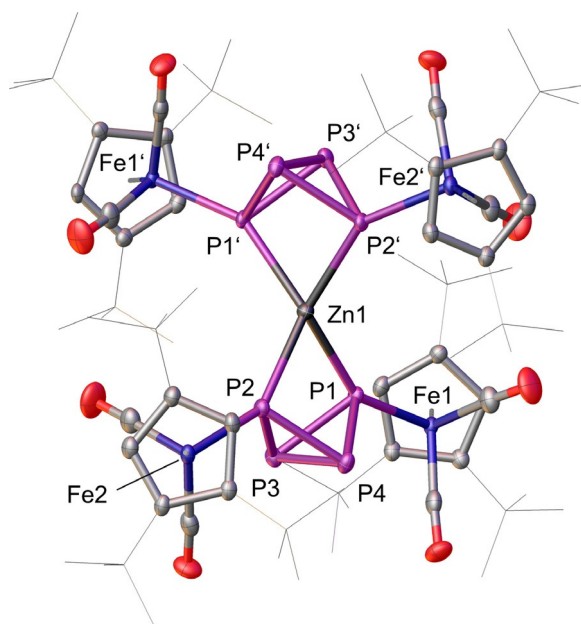


**Figure 5.** Cationic part of the molecular structure of **5**. The two  $\text{PF}_6^-$  anions, hydrogen atoms and solvent molecules are omitted for clarity. ADPs are shown at 50% probability level.

The  $^1\text{H}$  NMR spectrum ( $\text{CD}_2\text{Cl}_2$ ) of **5** shows the characteristic signals for the magnetically equivalent  $\text{Cp}^{\text{III}}$  ligands at  $\delta = 5.00$ , 1.45 and 1.42 ppm. The  $^{31}\text{P}\{^1\text{H}\}$  NMR spectrum ( $\text{CD}_2\text{Cl}_2$ ) of **5** reveals an  $\text{AA}'\text{A}''\text{A}'''\text{XX}'\text{X}''\text{X}'''$  spin system at  $\delta = -13.2$  and  $-295.3$  ppm (coupling constants are summarized in Table S8) for the cation and a septet at  $\delta = -143.8$  ppm for the two  $\text{PF}_6^-$  anions.

Moreover, we were also interested in whether **5** can also be formed starting from **2Zn**. Therefore, **2Zn** is treated with the halogen abstractor  $\text{Ti}[\text{PF}_6]$  in the presence of **1**. The quantitative formation of **5** was confirmed by  $^{31}\text{P}$  NMR spectroscopy.

## Conclusions

We have reported on the versatile coordination behavior of the butterfly complex **1**. On the one hand, **1** acts as a bidentate ligand for divalent bromide salts to give complexes **2Co**, **2Ni**, and **2Zn**. In these compounds the  $\text{P}_4$  butterfly unit coordinates the Lewis acids via the two “wing-tip” phosphorus atoms. Thereby, the exhibited bite angles are comparable to analogue dppm complexes. On the other hand, however, the formation of two unidentified side products, which exhibit an altered  $\text{P}_4$  scaffold and occur during the synthesis of **2Ni** and **2Zn**, indicates that complex **1** is electronically highly flexible. This behavior is especially emphasized in the reaction with  $[\text{Co}(\text{NCCH}_3)_6][\text{SbF}_6]_2$ , which leads to **3** as the second example of a homoleptic octaphospha-metal-sandwich complex. Here, the  $\text{P}_4$  ligands act as  $6\pi$ -electron donors, which is enabled by isomerization to aromatic *cyclo*- $\text{P}_4$  ligands. However, surprisingly the starting material  $[\text{Co}(\text{NCCH}_3)_6][\text{SbF}_6]_2$  gets at least partly oxidized from  $\text{Co}^{\text{II}}$  to  $\text{Co}^{\text{III}}$  which also leads to an unselective degradation of **1** and the formation of several byproducts, like the monocationic compound **4**, a product of a dimerization of

**1** in the presence of a  $[\text{Co}(\text{CO})_2]^{3+}$  fragment. Complex **4** contains a  $\text{P}_8$  unit which represents a rare all-phosphorus derivative of bicyclo[3.3.0]octane. The reaction of **1** and  $[\text{Zn}(\text{NCCH}_3)_4][\text{PF}_6]_2$  leads to the formation of the spiro complex **5** that still bears intact  $\text{P}_4$  butterfly units. However, this outcome highlights that the isomerization is not dependent on the nature of the ligand only, but also strongly related with electronic properties of the metal. Therefore, this study clearly shows that the rearrangement of **1** is feasible in the presence of weakly ligated  $d^6$  metals only.

## Experimental Section

**Crystallographic data:** Deposition numbers 2026542 (**2Co**), 2026543 (**2Ni**), 2026544 (**2Zn**), 2026545 (**3**), 2026546 (**4**), 2026547 (**5**), 2026548 ( $[\text{Cp}^{\text{III}}\text{Fe}(\text{CO})_3][\text{PF}_6]$ ), and 2026549 ( $[\text{Cp}^{\text{III}}\text{Fe}(\text{CO})_3][\text{SbF}_6]$ ) contain the supplementary crystallographic data for this paper. These data are provided free of charge by the joint Cambridge Crystallographic Data Centre and Fachinformationszentrum Karlsruhe Access Structures service.

## Acknowledgements

This work was supported by the Deutsche Forschungsgemeinschaft (Sche 384/38-1). We thank Martin Weber for the measurement and interpretation of the cyclic voltammograms. Open access funding enabled and organized by Projekt DEAL.

## Conflict of interest

The authors declare no conflict of interest.

**Keywords:** chelate ligands · *cyclo*- $\text{P}_4$  ligands ·  $\text{P}_4$  butterfly complexes ·  $\text{P}_4$  transformation · phosphorus

- [1] K. H. Whitmire, *Coord. Chem. Rev.* **2018**, *376*, 114.
- [2] J. A. Gillespie, D. L. Dodds, P. C. J. Kamer, *Dalton Trans.* **2010**, *39*, 2751.
- [3] S. M. Mansell, *Dalton Trans.* **2017**, *46*, 15157.
- [4] a) L.-S. Luh, U. B. Eke, L.-K. Liu, *Organometallics* **1995**, *14*, 440; b) Y. B. Malysheva, D. V. Moiseev, A. V. Gushchin, V. A. Dodonov, *Russ. J. Gen. Chem.* **2005**, *75*, 1766; c) D. V. Moiseev, Y. B. Malysheva, A. S. Shavirin, Y. A. Kurskii, A. V. Gushchin, *J. Organomet. Chem.* **2005**, *690*, 3652.
- [5] B. Gabor, S. Holle, P. W. Jolly, R. Mynott, *J. Organomet. Chem.* **1994**, *466*, 201.
- [6] S. M. Jing, V. Balasanthiran, V. Pagar, J. C. Gallucci, T. V. RajanBabu, *J. Am. Chem. Soc.* **2017**, *139*, 18034.
- [7] M. Schultz, F. Eisenträger, C. Regius, F. Rominger, P. Hanno-Igles, P. Jakob, I. Gruber, P. Hofmann, *Organometallics* **2012**, *31*, 207.
- [8] J. A. S. Bomfim, F. P. de Souza, C. A. L. Filgueiras, A. G. de Sousa, M. T. P. Gambardella, *Polyhedron* **2003**, *22*, 1567.
- [9] A. M. Messinis, S. L. J. Luckham, P. P. Wells, D. Gianolio, E. K. Gibson, H. M. O'Brien, H. A. Sparkes, S. A. Davis, J. Callison, D. Elorriaga, O. Hernandez-Fajardo, R. B. Bedford, *Nat. Catal.* **2019**, *2*, 123.
- [10] a) M.-N. Birkholz née Gensow, Z. Freixa, P. W. N. M. van Leeuwen, *Chem. Soc. Rev.* **2009**, *38*, 1099; b) P. W. N. M. van Leeuwen, P. C. J. Kamer, J. N. H. Reek, P. Dierkes, *Chem. Rev.* **2000**, *100*, 2741; c) P. Dierkes, P. W. N. M. van Leeuwen, *Dalton Trans.* **1999**, 1519.

- [11] V. Balema, H. Goesmann, E. Matern, G. Fritz, *Z. Anorg. Allg. Chem.* **1996**, 622, 35.
- [12] a) H. Binder, B. Schuster, W. Schwarz, K. W. Klinkhammer, *Z. Anorg. Allg. Chem.* **1999**, 625, 699; b) D. Bongert, H.-D. Hausen, W. Schwarz, G. Heckmann, H. Binder, *Z. Anorg. Allg. Chem.* **1996**, 622, 1167; c) S. Gómez-Ruiz, B. Gallego, E. Hey-Hawkins, *Dalton Trans.* **2009**, 2915; d) S. Gómez-Ruiz, R. Wolf, E. Hey-Hawkins, *Dalton Trans.* **2008**, 1982; e) K. Issleib, F. R. Krech, E. Lapp, *Synth. React. Inorg. Met. Org. Chem.* **1977**, 7, 253.
- [13] A. Forster, C. S. Cundy, M. Green, F. Stone, *Inorg. Nucl. Chem. Lett.* **1966**, 2, 233.
- [14] a) M. A. Bush, V. R. Cook, P. Woodward, *Chem. Commun. (London)* **1967**, 630; b) S. J. Geier, D. W. Stephan, *Chem. Commun.* **2008**, 2779; c) D. M. Yufanyi, T. Grell, E. Hey-Hawkins, *Eur. J. Inorg. Chem.* **2019**, 1557.
- [15] a) B. M. Cossairt, N. A. Piro, C. C. Cummins, *Chem. Rev.* **2010**, 110, 4164; b) M. Scheer, G. Balázs, A. Seitz, *Chem. Rev.* **2010**, 110, 4236; c) M. Caporali, L. Gonsalvi, A. Rossin, M. Peruzzini, *Chem. Rev.* **2010**, 110, 4178.
- [16] A. P. Ginsberg, W. E. Lindsell, *J. Am. Chem. Soc.* **1971**, 93, 2082.
- [17] I. Krossing, L. van Wüllen, *Chem. Eur. J.* **2002**, 8, 700.
- [18] a) S. Dürr, D. Ertler, U. Radius, *Inorg. Chem.* **2012**, 51, 3904; b) O. J. Scherer, M. Swarowsky, H. Swarowsky, G. Wolmershäuser, *Angew. Chem. Int. Ed. Engl.* **1988**, 27, 694; *Angew. Chem.* **1988**, 100, 738.
- [19] O. J. Scherer, T. Hilt, G. Wolmershäuser, *Organometallics* **1998**, 17, 4110.
- [20] O. J. Scherer, G. Schwarz, G. Wolmershäuser, *Z. Anorg. Allg. Chem.* **1996**, 622, 951.
- [21] a) S. Pelties, D. Herrmann, B. de Bruin, F. Hartl, R. Wolf, *Chem. Commun.* **2014**, 50, 7014; b) S. Heintl, M. Scheer, *Chem. Sci.* **2014**, 5, 3221.
- [22] C. Schwarzmaier, A. Y. Timoshkin, G. Balázs, M. Scheer, *Angew. Chem. Int. Ed.* **2014**, 53, 9077; *Angew. Chem.* **2014**, 126, 9223.
- [23] C. Schwarzmaier, S. Heintl, G. Balázs, M. Scheer, *Angew. Chem. Int. Ed.* **2015**, 54, 13116; *Angew. Chem.* **2015**, 127, 13309.
- [24] J. Müller, S. Heintl, C. Schwarzmaier, G. Balázs, M. Keilwerth, K. Meyer, M. Scheer, *Angew. Chem. Int. Ed.* **2017**, 56, 7312; *Angew. Chem.* **2017**, 129, 7418.
- [25] P. Pyykkö, M. Atsumi, *Chem. Eur. J.* **2009**, 15, 186.
- [26] These signals were mistakenly assigned to  $[(\text{Cp}^*\text{Fe}(\text{CO})_2)_2(\mu_3, \eta^{2:1:1}\text{P}_4)\{\text{Cp}^*\text{Fe}(\text{CO})\}]^+$  in the previous work.
- [27] a) D. F. Evans, *J. Chem. Soc.* **1959**, 2003; b) G. A. Bain, J. F. Berry, *J. Chem. Educ.* **2008**, 85, 532.
- [28] B. N. Figgis, R. S. Nyholm, *J. Chem. Soc.* **1954**, 12.
- [29] A. B. P. Lever, *Inorg. Chem.* **1965**, 4, 763.
- [30] a) C. Ercolani, J. V. Quagliano, L. M. Vallarino, *Inorganica Chim. Acta* **1973**, 7, 413; b) G. R. van Hecke, W. D. Horrocks, *Inorg. Chem.* **1966**, 5, 1968.
- [31] P. Pyykkö, M. Atsumi, *Chem. Eur. J.* **2009**, 15, 12770.
- [32] a) A. Cavaillé, N. Saffon-Merceron, N. Nebra, M. Fustier-Boutignon, N. Mézailles, *Angew. Chem. Int. Ed.* **2018**, 57, 1874; *Angew. Chem.* **2018**, 130, 1892; b) U. Chakraborty, J. Leitl, B. Muhldorf, M. Bodensteiner, S. Pelties, R. Wolf, *Dalton Trans.* **2018**, 47, 3693; c) F. Dielmann, A. Timoshkin, M. Piesch, G. Balázs, M. Scheer, *Angew. Chem. Int. Ed.* **2017**, 56, 1671; *Angew. Chem.* **2017**, 129, 1693; d) M. Modl, S. Heintl, G. Balázs, F. Delgado Calvo, M. Caporali, G. Manca, M. Keilwerth, K. Meyer, M. Peruzzini, M. Scheer, *Chem. Eur. J.* **2019**, 25, 6300; e) M. Piesch, S. Reichl, M. Seidl, G. Balázs, M. Scheer, *Angew. Chem. Int. Ed.* **2019**, 58, 16563; *Angew. Chem.* **2019**, 131, 16716; f) O. J. Scherer, R. Winter, G. Wolmershäuser, *Z. Anorg. Allg. Chem.* **1993**, 619, 827.
- [33] F. Kraus, J. C. Aschenbrenner, N. Korber, *Angew. Chem. Int. Ed.* **2003**, 42, 4030; *Angew. Chem.* **2003**, 115, 4162.
- [34] Z. Li, C. Zhao, L. Chen, *J. Mol. Struct.* **2007**, 810, 1.
- [35] M. Piesch, M. Seidl, M. Scheer, *Chem. Sci.* **2020**, 11, 6745.
- [36] D. A. Dickie, R. A. Kemp, *Organometallics* **2014**, 33, 6511.

---

Manuscript received: November 19, 2020

Accepted manuscript online: December 14, 2020

Version of record online: January 25, 2021